Journal of Energy, Environmental & Chemical Engineering
2022; 7(3): 90-101
http://www.sciencepublishinggroup.com/j/jeece
doi: 10.11648/j.jeece.20220703.16
ISSN: 2637-4331 (Print); ISSN: 2637-434X (Online)

Synthesis and Characterization of Cellulose Nanocrystals from Water Hyacinth Using Acid Hydrolysis

Muluneh Ayalew Balcha[1], Girma Gonfa Hunde[2], Muleta Ali Wakjira[1], Nedumaran Balasubramanian[1, *]

[1]Department of Chemical Engineering, College of Engineering and Technology, Bule Hora University, Bule Hora, Ethiopia

[2]Department of Chemical Engineering, Biotechnology and Bioprocess Center of Excellence, Addis Ababa Science and Technology University, Addis Ababa, Ethiopia

Email address:

muluneh.ayalew@bhu.edu.et (Muluneh Ayalew Balcha), kiyaagonfaa@gmail.com (Girma Gonfa Hunde), alimuler2020@gmail.com (Muleta Ali Wakjira), bnedumaran@gmail.com (Nedumaran Balasubramanian)

[*]Corresponding author

To cite this article:

Muluneh Ayalew Balcha, Girma Gonfa Hunde, Muleta Ali Wakjira, Nedumaran Balasubramanian. Synthesis and Characterization of Cellulose Nanocrystals from Water Hyacinth Using Acid Hydrolysis. *Journal of Energy, Environmental & Chemical Engineering*. Vol. 7, No. 3, 2022, pp. 90-101. doi: 10.11648/j.jeece.20220703.16

Received: August 14, 2022; **Accepted**: September 16, 2022; **Published**: September 29, 2022

Abstract: Water hyacinth (WH) is a widespread aquatic plant with extremely high growth rate which pose a threat in the past and great challenge due to its ability to rapidly cover the whole water body, leading to phytoplankton. Biological, physical and chemical methods have been tried resulting into high cost and labor requirements, for the control and eradication of this plant from water bodies. The aim of this study was to utilize this plant for production of cellulose nanocrystals (CNCs) using hydrolysis with sulphuric acid at varying values of reaction temperature, time and acid concentration. Pre-treatment steps such as soxhlet extraction, alkaline treatment and bleaching were performed for successful isolation of cellulose for acid hydrolysis. After acid hydrolysis, purified dispersion of CNCs was obtained using successive centrifugation, dialysis and ultra-sonication. The effect of process parameters on the yield of CNCs was evaluated and optimized using response surface methodology (RSM). The raw WH, freeze dried cellulose and CNCs samples were characterized using scanning electron microscopy, X-ray diffraction, Fourier Transform Infrared Radiation, differential scanning calorimetry and particle size analyzer. It was found that the whisker-shaped structured CNCs was isolated with an average diameter of 102.6 nm and showing high thermal stability. It was also observed that the non-cellulosic components were successfully removed and the crystallinity index as well as crystal thickness of the sample was improved after each treatment. The yield of CNCs was affected by selected process parameters and the maximum yield of 37.72% was obtained at 50°C, 35 min and 54% acid concentration and optimized to 38.4057%.

Keywords: Water Hyacinth, Sulphuric Acid, Cellulose Nanocrystals, Hydrolysis

1. Introduction

The development of sustainable and eco-friendly materials derived from renewable sources (biomass) has gained the attention of researchers [1-3]. Lignocellulosic biomass is the most abundantly available renewable raw materials ideal for replacing oil-based feedstocks [2-4]. Cellulose nanocrystals (CNCs) are an interesting material among cellulose material for different applications due to its attractive properties [5-7]. The specific properties of cellulose nanocrystalline includes excellent mechanical properties, high surface to volume ratio, light weight, low density, rich hydroxyl groups for modification, a capacity to be acquired in different dimension such as aspect ratio, inexhaustibility and natural properties with 100% environmental [7-10]. The surface of CNCs can be modified with various chemical treatments to any desired surface modification due to the abundant hydroxyl groups on the surface of CNCs which provide them reactive sites [11]. This can successfully functionalize the CNCs and facilitate the incorporation and dispersion of CNCs into different polymer matrices [10, 12, 13]. CNCs applications includes a barrier in the separation process of hazardous waste,

biomedical products, electronic sensors, paints and coatings, as the thickener in cosmetics, biodegradable package, CO_2 adsorbent, as filler of special textiles, food wraps and texturing agent which replace the non-biodegradable plastics, as fillers and rheology modifiers in different fields like foams, aerogels and polymer electrolytes [3, 13-16]. The lignocellulosic biomass may include higher plants, agricultural residues, certain micro-organisms certain animals from which cellulose can be extracted [7, 12, 17]. However, most of these lignocellulosic biomasses are obtained from seasonable and slow growing plants as well as utilizing for other purposes [18]. The extractions of CNCs from agricultural residue such as garlic straw residues [1], sugarcane bagasse [6, 10], cotton linter [5], lotus leaf stalk [18], tomato peels [19], and pineapple [20] have been investigated. In the current work, CNCs was extracted from water hyacinth (WH). WH is one of lignocellulosic biomasses that can be used as a suitable feedstock for cellulose nanocrystals [9, 21-28]. WH has extremely high growth rates and called the world's worst aquatic weed due to its ability to rapidly cover whole waterways [29]. This leads to the formation of dense coverage that prevents the sunlight from penetrating the water and impenetrable mats over the water surface [27]. It can also forms other specific problems such as destruction of eco systems, blocking irrigation channels and rivers, destroying natural wetlands, eliminating native aquatic plants, reducing infiltration of sunlight, changing the temperature, pH and oxygen levels of water, reducing gas exchange at the water surface, increasing water loss through transpiration, restricting recreational use of waterways, and reducing water quality from decomposing plants, leading to phytoplankton effect [28, 30]. The negative effects of WH lead to several research and developmental activities for the control of this notorious weed [29]. Although different methods such as biological, physical and chemical methods have been tried for the control and eradication of WH, none of these strategies proved to be a permanent solution since the attempts to control this weed have high costs and labour requirements [27, 29]. Thus, it is necessary to find a suitable way to utilize the WH, that is, by mechanically removing it from water bodies and producing value added materials from it. WH has a high percentage of cellulose which is comparable with the fiber content from other sources, such as wood, rise husk, wheat straw, corn strove, and pineapple leaf [9, 23, 25, 31]. This shows WH can be used as feedstock for production cellulose or nanocellulose based materials. The use of WH as feedstock gives a twofold advantage. First, it reduces the environmental problem caused by it. Second, conversion of WH to value added products has significant economic importance.

Different methods such as mechanical treatment, biological treatment (enzymatic hydrolysis), chemical treatment (acid hydrolysis), and the combination of any of these methods can be used to produce nanocellulose from lignocellulosic biomass [16, 17, 6, 30]. All these treatment methods lead to the different types of nanostructured cellulose molecules differing in dimension, degree of crystallinity and morphologies depending on their disintegration process and feedstocks [15]. However, high energy is required for the mechanical method and longtime of operation and high cost is needed for enzymatic hydrolysis. Acid hydrolysis was used for cost effectiveness and high efficiency to obtain cellulose nanocrystals, that has better properties such as with higher crystallinity index and smaller size than other methods [33, 34]. During acid hydrolysis, the most important factors to be controlled are acid concentration, reaction time and reaction temperature [35]. Different acids have been used for acid hydrolysis of lignocellulosic fibers. Among different acid used, sulfuric acid (H_2SO_4) and hydrochloric acid (HCl) are the most common for hydrolysis purpose [7, 15]. However, treatment with hydrochloric acid results in reduced dispersion of crystals, leading to flocculation in solution, lower crystallinity index due to its higher tendency to promote the breakage of the hydrogen bonds in the crystalline region of cellulose [7]. H_2SO_4 is the most common acid used for acid hydrolysis process since it produces CNCs particles grafted with the negatively charged sulfate ester group which makes the CNCs particles a negative electrostatic repulsion force. It stabilizes the nanocellulose suspension by electrostatic repulsion avoiding fibril aggregation [7, 14, 36]. In this study, cellulose nanocrystals were synthesized from WH using H_2SO_4 hydrolysis method and the effects of reaction temperature, reaction time and acid concentration on the yield of CNCs were investigated and optimized using Response Surface Method (RSM). Characterization of CNCs was performed with different techniques.

2. Experimental

2.1. Materials

The reagents and chemicals used in this study were toluene (99%), ethanol (97%), sodium hydroxide (97%), sodium hypochlorite, distilled water, acetic acid (99.5%), sulfuric acid (95%), and chloroform (99%). All the chemicals used in experiments were of analytical grade.

2.2. Methods

2.2.1. Isolation of Cellulose

WH was collected from nearby waterbody (Koka dam) by mechanical means. The WH stems were separated from its leaves and roots using laboratory knife, washed with distilled water to remove dusts and then dried in an oven at the temperature of 60°C for 24 h [15]. The dried sample was chopped, milled and sieved using 60-mesh sieve to get the powder form of sample. Next, the sample was dewaxed in a soxhlet apparatus using mixture of toluene and ethanol solvents with the ratio of 2:1 (v/v) [18]. The de-waxing was conducted at 85°C for 5 h to remove extractive components such as wax, pectin and oils. The de-waxed powder was washed with distilled water and ethanol using 45 μm sieve to remove solvent and finally dried in oven at 45°C. The dewaxed sample was treated twice in autoclave reactor

(HPA-1L) with 4% (w/w) NaOH solutions with a ratio of 1:20 (g/ml) at 80°C for 2 h under constant agitation at 500 rpm [30]. The treated sample was thoroughly neutralized using diluted acetic acid and distilled water. Then, the sediment obtained from centrifugation was dried in tray drier (TDC/EV) at 45°C to constant weight. After alkaline treatment, the dried sample was bleached using a mixture of 6% (w/w) sodium hypochlorite solutions and acetic acid with the ratio of 4:1 (v/v) under acidic condition (pH 4) to remove lignin [15, 30]. The bleached sample was cooled in reactor by using chiller connected with reactor. Then, it was washed repeatedly with diluted solution of sodium hydroxide and distilled water until free from acid and to achieve neutral pH. During washing step, the successive centrifugation was performed by replacing supernatant with distilled water until white cellulose was obtained. Finally, the obtained white cellulose was frozen using deep freezer and then freeze dried to obtain powder cellulose and preserved in a sealed plastic bag for further analysis.

2.2.2. Preparation of Cellulose Nanocrystals

A controlled H_2SO_4 hydrolysis was performed in autoclave reactor to split the amorphous domains, remove local inter fibril crystalline contacts of the pretreated sample. Purified cellulose was acid hydrolyzed using 10g of cellulose in 250 ml of sulfuric acid under controlled conditions and continuous agitation at 500 rpm [23]. The hydrolysis reaction was stopped by quenching with ice to. The hydrolyzed cellulose sample was then washed repeatedly with successive centrifugation at 4000 rpm for 25 min to remove excess sulfuric acids [30]. The suspension was then dialyzed against deionized water using cellulose membrane for 4 days to neutralize and fully remove free acid molecules, non-reactive sulfate group, salts and soluble sugars. After dialysis, the suspension of CNCs was ultra-sonicated for 15 min to get aqueous homogenized dispersion and labeled as the CNCs suspension [30, 32]. A few drops of chloroform were added to the freshly prepared suspension to prevent degradation of the cellulose nanocrystals and then stored in refrigerator at 4°C for characterization. The yield of dried CNCs was calculated as shown in (1):

$$Y(\%) = W_1/W_2 \times 100 \quad (1)$$

where, Y represents yield, W_1 and W_2 represents weight of CNCs obtained after hydrolysis and that of cellulose before hydrolysis on dry basis.

2.2.3. Experimental Design

The effects of three factors on the yield of CNCs were investigated using the response surface methodology based on box-Behnken design (BBD). Each factor consisted of three levels such that temperature (40, 50, 60)°C, time (30, 45, 60) min and acid concentration (50, 57.5, 65)%. A total of 15 experiments were designed and conducted in random order. A second-order polynomial empirical model was used for the yield (Eq. (2)).

$$Y = \beta_0 + \sum \beta_i X_i + \sum \beta_i X_i^2 + \sum \beta_i X_i X_j \quad (2)$$

Analysis of variance (ANOVA) was used to check the adequacy of the model for the responses in the experimentation. Box-plots of three factors, 2D contour plots, 3D response surface plots and one factor and two factor interaction plots were used for the analysis.

2.3. Characterizations

2.3.1. Particle Size Determination

Particle size distribution of CNCs was measured using Malvern Zetasizer nano (ZE3600). Sample suspension was diluted with distilled water and analyzed at 25°C with a calibration time of 2 min. The particle size is determined by measuring the random changes in the intensity of light scattered from a suspension. Malvern Zetasizer software (version 7.12) was used.

2.3.2. Fourier Transform Infrared Spectroscopy

Fourier Transform Infra-red Spectrometer (FTIR) was used for studying change of functional groups present in the materials before and after their production process. Dried powder of WH, cellulose and CNCs samples were tested and the spectra of the samples were recorded over range of 4000 to 400 cm^{-1} wave number using FTIR (Thermo Scientific iS50 ABX).

2.3.3. Scanning Electron Microscopy Studies (SEM)

The morphological analysis of WH, bleached cellulose and CNCs was performed using Scanning Electron Microscopy (FEI INSPECT F50 model).

2.3.4. X-ray Diffraction (XRD)

The change in crystallinity index and crystal thickness of the samples from raw WH to CNCs was evaluated by X-ray diffraction patterns. The powder of WH, bleached cellulose and CNCs samples were scanned at room temperature with diffraction angle in the range of 5° to 80° and a step size of 0.03°. Then the crystallinity index of the analyzed samples was calculated through the Segal's equation [33] at scanning rate of 0.5°/min.

Crystallinity index:

$$C_I = \left[\frac{I_{200} - I_{am}}{I_{200}}\right] \times 100 \quad (3)$$

where, I_{200} is the maximum diffraction intensity values of crystalline at a 2θ ranged from 52.5° to 57.5° cellulose and I_{am} shows minimum intensity value of amorphous cellulose at 2θ ranged from 37.5° to 40°. Similarly, the crystal thickness (D) measured using Derby Scherer's equation at a given d-spacing [34].

$$D = \frac{k\lambda}{\beta \cos\theta} \quad (4)$$

where, k is for factor with value of 0.9, λ is a constant wave length of 0.1574 nm, and β is the line width in radians at half the maximum intensity of I_{200} to which the background and the amorphous component have been subtracted, and is the scattering angle of the peak (2 0 0).

2.3.5. Differential Scanning Calorimetry (DSC)

DSC analysis were performed to see thermal behavior of raw WH, bleached cellulose and CNCs samples using Differential Scanning Calorimetry (SKZ1052B). Samples (4 mg of each) were placed in platinum crucible and heated from room temperature to 400°C for 40 min at heating rate of 10°C/min.

3. Results and Discussion

3.1. Scanning Electron Microscopy Analysis (SEM)

The morphology of WH, bleached cellulose and CNCs obtained were examined by SEM analysis as shown in Figure 1. The morphology and dimension of the fibers are found to be affected by the chemical treatment. Figure 1(A) shows the SEM image of the raw fiber. The surface of WH fiber was smooth before chemical treatments and became rougher after chemical treatments [35]. This shows the breaking of binding bonds formed by hemicellulose and lignin in natural fiber. The binding bonds are removed and thereby fibers get detached from the surface by the alkali treatment (Figure 1(B)). Figure 1 (C and D) clearly shows the defibrillation of fibers occurring during acid hydrolysis. The Figure shows that the extracted CNCs have a whisker-shaped structure which confirms their successful extraction from the WH [17, 23].

3.2. Fourier Transform Infrared Radiation (FTIR) Analysis

The FT-IR spectroscopy was done for studying the changes in the chemical structures after the various treatments of fibers. FTIR analysis of WH, bleached cellulose and CNCs samples are shown in Figure 2. In the spectrum of WH and CNCs, there were the peaks appeared at around 3734 cm^{-1} and 3614 cm^{-1} due to the presence of free O-H stretching sharp peak vibration [33]. This OH group attributed to adsorbed water and aliphatic alcohols that can found in hemicellulose, cellulose and other extractive components. The peak at 1032 cm^{-1} is appeared due to C-O stretch which can provide information about alcohol structure in raw sample. The intensity of this peak was gradually increased from raw WH to CNC, indicating that the cellulose content was increased during different chemical treatments. The FTIR spectrum of raw WH shows a characteristic peak at 1527.86 cm^{-1} and 2346.92 cm^{-1} which are associated with the stretching vibration of N-H band of the protein amide structure as well as N-O stretching of nitro compounds and O=C=O stretching of carbon dioxide, respectively [34]. This peak disappeared in the case of CNCs which indicates the elimination of protein and lignin molecules after acid hydrolysis. The observed peaks at around 1032 cm^{-1} and 1034 cm^{-1} are associated with the presence of S=O stretching sulfoxide groups in raw WH and CNCs due to acid hydrolysis. The peaks found at 2285.43 cm^{-1} and 2187.14 cm^{-1} in the case of cellulose indicates the presence of weak C≡N stretching of nitrile and weak C≡C stretching of alkyne group, respectively [36]. These peaks indicate the presence of carbonyl linkage (aromatic ring) in lignin and disappeared after acid hydrolysis. Similarly, the peak appeared at around 2000 cm^{-1} for cellulose sample shows the presence of triple bond groups such as weak H-C bending as well as C=C=C stretching of aromatic compounds. The spectra appeared in the range of 3000 to 2850 cm^{-1} due to C-H stretching for alkenes and aromatics [36]. The peaks appeared in the range of 1300 to 1000 cm^{-1} indicates the presence of ester with strong absorption due to the C-O bands. In CNCs the peaks found at 1690.86 and 1524.63 cm^{-1} indicates the presence of C=O stretching of conjugated aldehydes and strong N-O stretching of nitro compounds, respectively [30]. There is also one peak appeared at around 670 cm^{-1} which shows the presence of strong C=C bending of alkene in CNCs sample.

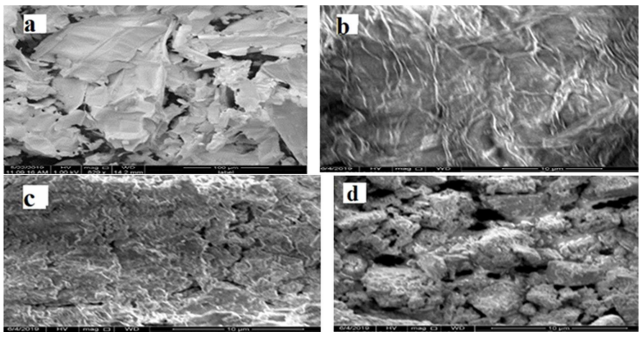

Figure 1. *SEM Image of raw WH (A), cellulose after bleaching (B) and CNCs (C, D).*

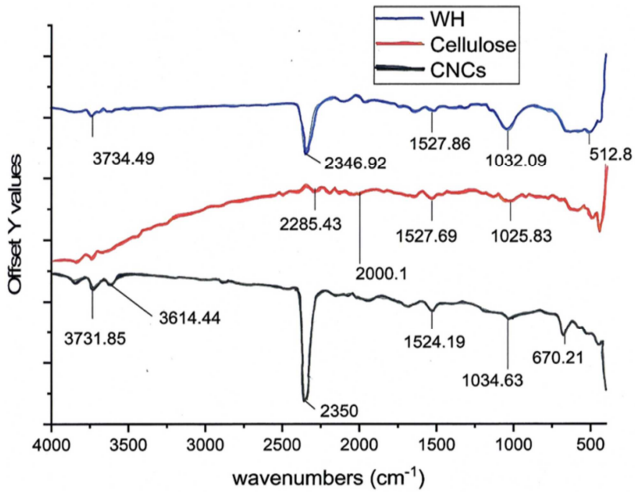

Figure 2. *FTIR spectra of WH, bleached cellulose and CNCs.*

3.3. X-ray Diffraction (XRD) Analysis

The crystalline structure and crystallinity index of WH, bleached cellulose and CNCs samples were analyzed by X-ray diffraction is shown in Figure 3. Along with small shift in peak position, the XRD profiles for samples are similar indicating that all samples contain cellulose. However, it is observed that there was a change in the relative intensity of the amorphous peaks and its width indicating a change in the crystallinity. The diffraction peak for raw WH was relatively broader and became sharper and narrower after chemical treatments. This indicates that the content of cellulose and degree of crystallinity was increased by chemical treatments.

The crystallinity index and crystal thickness of WH, bleached cellulose and CNCs samples were determined from Segal's and Scherer's equation [28] and given in Table 1. From this result, it can be observed that the crystallinity index and crystal thickness of the analysed samples was improved through chemical treatments due to successful removal of non-cellulosic components and amorphous part of obtained cellulose.

Table 1. *Crystallinity index and crystal thickness at different treatment stages.*

Samples	Crystallinity index (%)	Crystal thickness (nm)	d-spacing (nm)
WH	18	0.016	0.1034
Bleached cellulose	59	0.115	0.1427
CNCs	78	0.178	0.1789

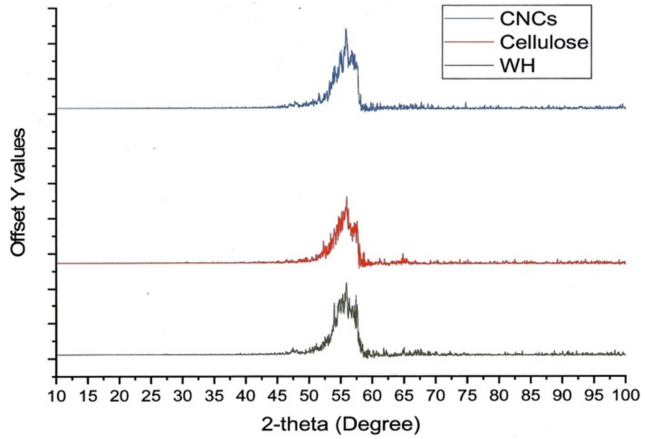

Figure 3. *X-ray diffraction patterns of raw WH, bleached cellulose, and CNCs.*

3.4. Particle Size Analysis

Particle size analysis was performed Zetasizer nano (ZE3600) to determine the mean average of size. Figure 4 shows the particle size distribution for CNCs indicating an average particle size (diameter) of 102.6 nm at measurement position 4.65 and count rate of 328.2 (kcps). It was observed that one major peak was recorded with average particle size of 102.6 at 100% intensity. As it can be seen from the Figure 4(a) and (b), the size distribution of CNCs particles was ranging from 50.75 nm to 190.1 nm in diameter. Size distribution by volume data shows that CNCs particle with smaller size of 50.75 nm accountable for 1.5% of volume while the particle with larger diameter of 190.1 nm accountable for 1.8% volume. The CNCs particles with average diameter of 102.6 nm accountable for around 19% of volume.

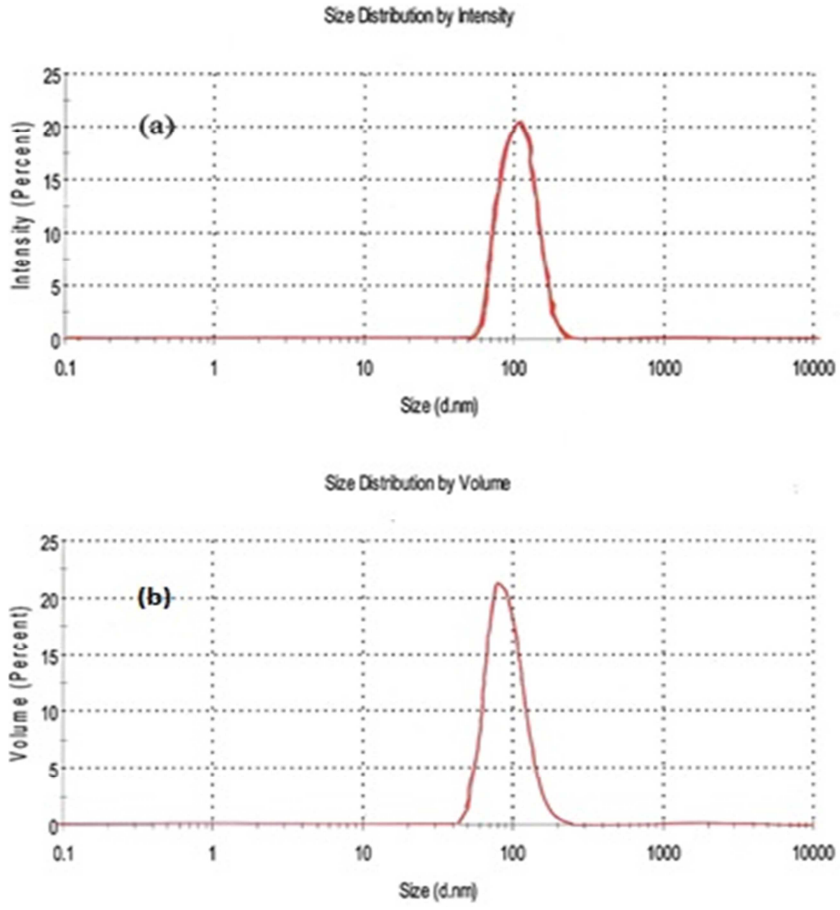

Figure 4. *Particle size distribution by intensity and volume; (a) based on peak intensity, (b) based on volume distribution.*

3.5. Differential Scanning Calorimetry (DSC)

The thermal behavior of raw WH, bleached cellulose and CNCs were analyzed using differential scanning calorimeter. Figure 5 shows the thermograms of DSC for analyzed samples. As it can be seen from the Figure, an endothermic peak was present in all thermograms at temperature range from 25°C to 100°C due to water loss by evaporation [15, 18, 23]. Other endothermic peaks observed on the thermograms indicates the melting point and decomposition of the samples. From the thermograms shown in Figure 5, it is observed that the position of the peaks increased after chemical treatment and higher for CNCs. This indicates that the amorphous part was decreased and the cellulose crystallite enhanced by chemical treatment. It is also observed that WH has a glass transition point at around 115°C to 150°C and for cellulose it was occurred at around 180°C to 210°C [22, 23]. The exothermic peaks found in all thermograms curves shows the decomposition point of the samples. WH degraded at around 275°C which is lower than that of cellulose and CNCs. This indicates the presence of impurities in raw material and removed after chemical treatment. Cellulose decomposed at around 325°C implying the successful removal of impurities and for CNCs it was occurred at temperature range of 350°C to 390°C. Generally, the result obtained from thermograms of DSC confirms that CNCs has high thermal stability and it been affected by chemical treatment.

3.6. Response Surface Methodology (RSM) Analysis

Fifteen experiments were performed according to the BBD. Analysis was done using DesignExpert V13 of StatEase software, to fit the response function. A second order polynomial model was found to be adequate for the prediction of the given yield as shown by equation (5):

$$Y = 37.71 - 1.9A - 2.58B - 0.7C - 2.46AB + 0.57AC - 0.22BC - 2.49A^2 - 2.26B^2 - 3.66C^2 \quad (5)$$

where, Y is the cellulose nanocrystals yield in percent, A, B and C stands for hydrolysis temperature, time and acid concentration respectively. All variables are indicated through the coded values. As suggested by the model F value (17132.79) and low probability value (p-value = 0.0001) which is less than 0.05, it is evidenced that the model is highly significant for this study as shown in Table 2. Multiple regression coefficients R^2 is 0.998. Figure 6, shows the relationship between the normal probability (%) and the internally studentized residuals. The straight line means that no response transformation was required and that there was no apparent problem with normality. Table 3 shows the experimental CNCs yield and the predicted values from RSM.

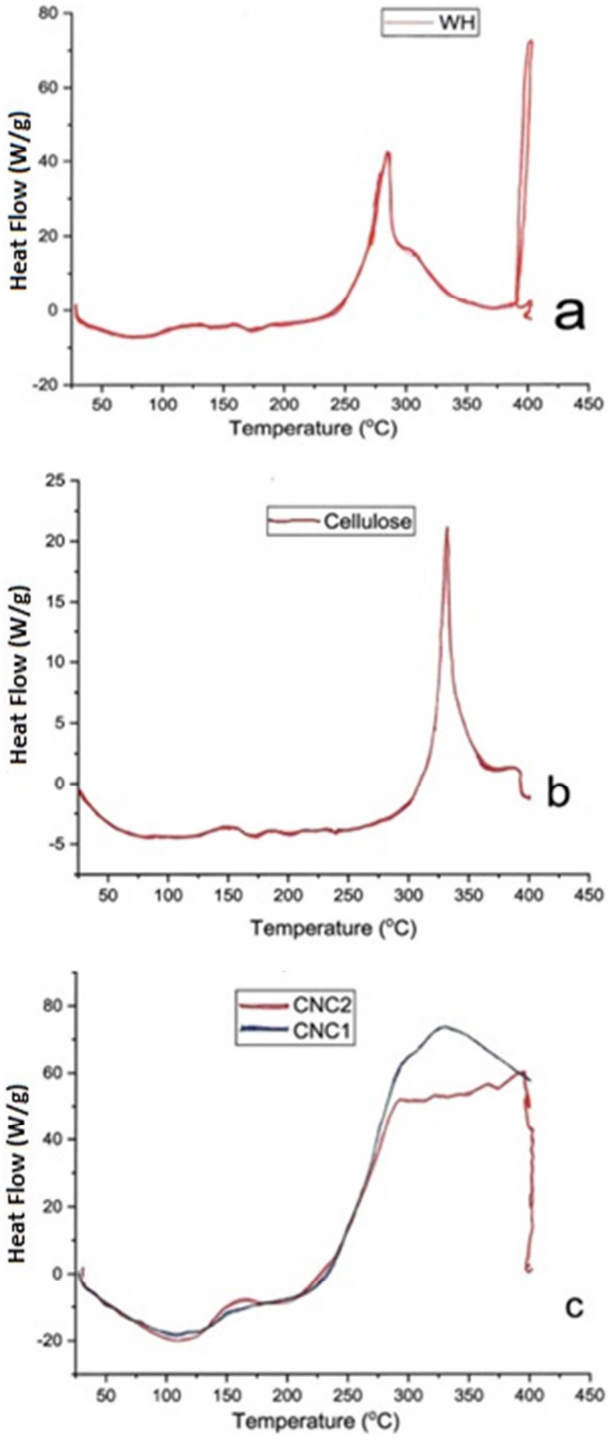

Figure 5. *DSC thermograms for (a) WH, (b) bleached cellulose and (c) CNCs.*

Table 2. *ANOVA Table.*

Source	Sum of Squares	df	Mean Square	F-value	p-value	
Model	191.72	9	21.30	17132.79	< 0.0001	*
A-A	28.88	1	28.88	23227.88	< 0.0001	
Model	53.25	1	53.25	42829.38	< 0.0001	
C-C	3.86	1	3.86	3107.94	< 0.0001	

Source	Sum of Squares	df	Mean Square	F-value	p-value	
AB	24.26	1	24.26	19508.55	< 0.0001	
AC	1.29	1	1.29	1036.11	< 0.0001	
BC	0.1892	1	0.1892	152.19	< 0.0001	
A^2	22.84	1	22.84	18369.23	< 0.0001	
B^2	18.89	1	18.89	15195.94	< 0.0001	
C^2	49.52	1	49.52	39826.01	< 0.0001	
Residual	0.0062	5	0.0012			
Lack of Fit	0.0057	3	0.0019	8.21	0.1105	**
Pure Error	0.0005	2	0.0002			
Cor Total	191.72	14				

*Significant, ** not significant

3.7. Effects of Parameters on the Yield of Crystalline Nanocellulose

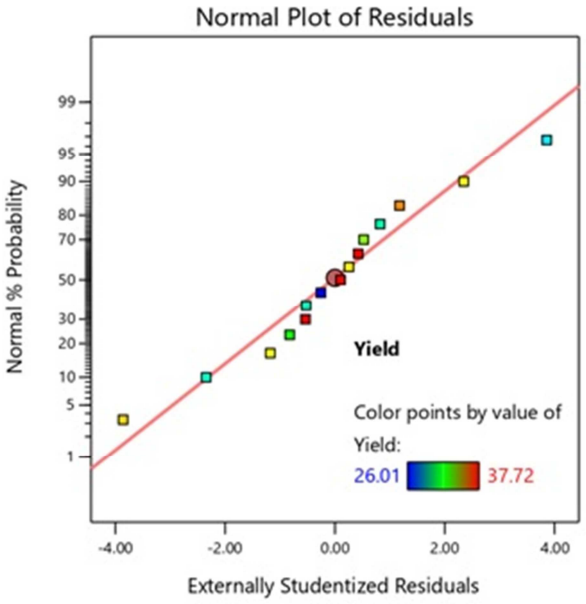

Figure 6. *Normal plot of residuals experimental values.*

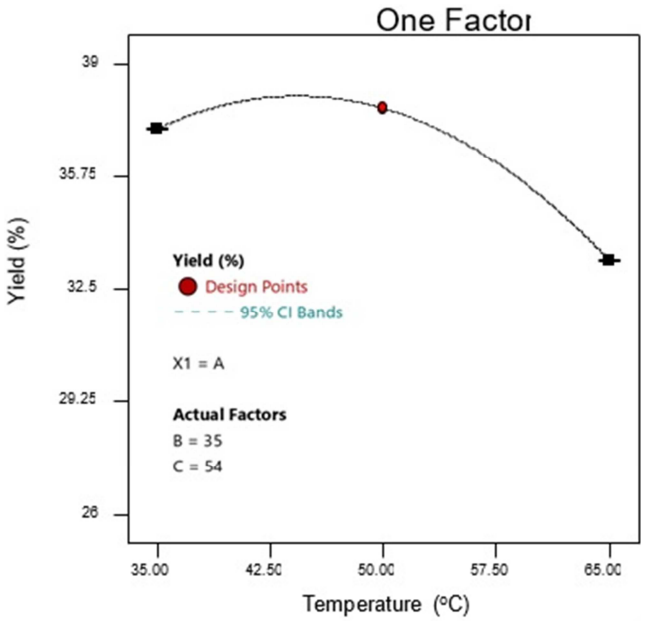

Figure 7. *Effect of temperature on response at constant time and acid concentration.*

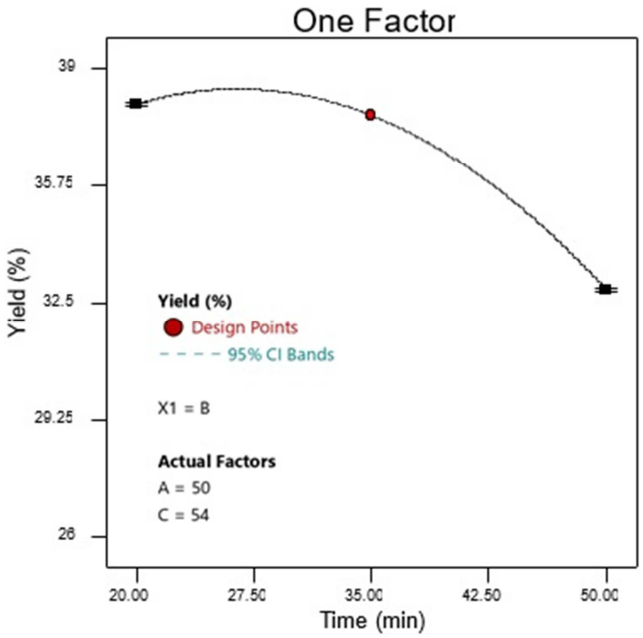

Figure 8. *Effect of hydrolysis time on the yield of CNCs.*

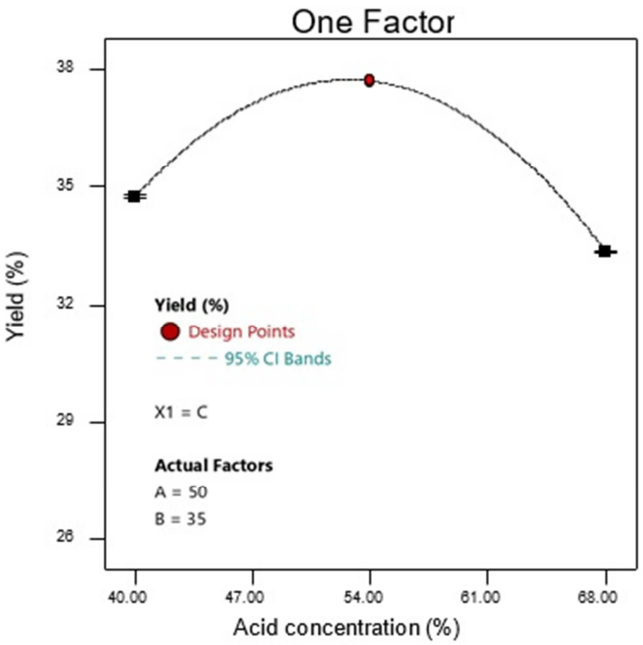

Figure 9. *Effect of acid concentration on the yield of CNCs.*

Table 3. *BBD matrix of independent variables used in RSM with corresponding experimental and predicted values of response.*

Std	Run	Factors			Yield (%)	
		T (°C)	Time (min)	Acid con. (%)	Exp.	Pred.
15	1	50.00	35.00	54.00	37.72	37.71
1	2	35.00	20.00	54.00	34.98	34.97
11	3	50.00	20.00	68.00	33.46	33.45
9	4	50.00	20.00	40.00	35.24	35.27
2	5	65.00	20.00	54.00	36.12	36.10
7	6	35.00	35.00	68.00	32.18	32.19
8	7	65.00	35.00	68.00	29.5	29.53
4	8	65.00	50.00	54.00	26.01	26.02
13	9	50.00	35.00	54.00	37.71	37.71
12	10	50.00	50.00	68.00	28.76	28.73
6	11	65.00	35.00	40.00	29.8	29.79
10	12	50.00	50.00	40.00	29.67	29.68
14	13	50.00	35.00	54.00	37.69	37.71
3	14	35.00	50.00	54.00	34.72	34.74
5	15	35.00	35.00	40.00	34.75	34.72

3.7.1. Effects of One Factor

Figure 7 shows the individual effects of hydrolysis temperature on the response of the study by keeping other two parameters at their values that gives the maximum yield. It was observed that at the lower level of temperature, the yield is increased with increasing the temperature since the hydrolysis reaction is non-isothermal.

After it reaches the optimum value of 50°C, further increasing the temperature lower the values of the yield due to the degradation of cellulose. The negative value of regression coefficient of temperature indicates how the temperature negatively affect the response after optimum point and agrees with the relation shown by (5). Similar behaviour was observed with respect to time, (Figure 8) indicating the reaction rate is high at the beginning of the reaction and prolonged reaction time leads to undesired degradation of product. As shown in Figure 9, lower concentration favors the yield of CNCs and degrades the product with increased concentration. The yield reaches its optimum at acid concentration of 54% and then decreased with further increasing of acid concentration due to the over degradation of cellulose to undesired products.

3.7.2. Interaction Effect of Two Factors

The combined interaction of temperature and time (Figure 10), temperature and acid concentration (Figure 11) and time and acid concentration (Figure 12) are negatively affect the yield of CNCs. It was observed that the yield was increased with increasing temperature and time and less significant on acid concentration. This happened due to the over degradation of cellulose to undesired products at higher level of both temperature and time. The interaction of temperature and acid concentration has higher effect on the yield than other possible interaction.

3.7.3. Response Surface and Contour Plot

Figure 13 shows the effect of temperature and time on the yield of CNCs at fixed value of acid concentration. It was observed that the yield of CNCs increased with increasing hydrolysis time to 35 min and the temperature to 50°C at which the optimum yield was obtained. At the higher-level temperature and time, the yield was lower due to the over degradation of cellulose to undesired products. Figure 14 shows the effect of temperature and acid concentration at a fixed value of acid concentration. From Figure 14, it was observed that the yield of CNC was increased with increasing acid concentration to 54% and temperature to 50°C at which the optimum yield was obtained. However, further increasing of both acid concentration and temperature results in the decrement of CNCs yield due to the over degradation of cellulose to undesired products. concentration. At higher level of acid concentration and time the cellulose molecules can undergo over degradation to undesired products.

Figure 15 shows the response surface plot with the interaction effect of time and acid concentration at affixed value of temperature. It was observed that the yield was increased with increasing acid concentration and time at them meddle values at which the optimum yield was obtained and decreased with further increasing of hydrolysis time and acid.

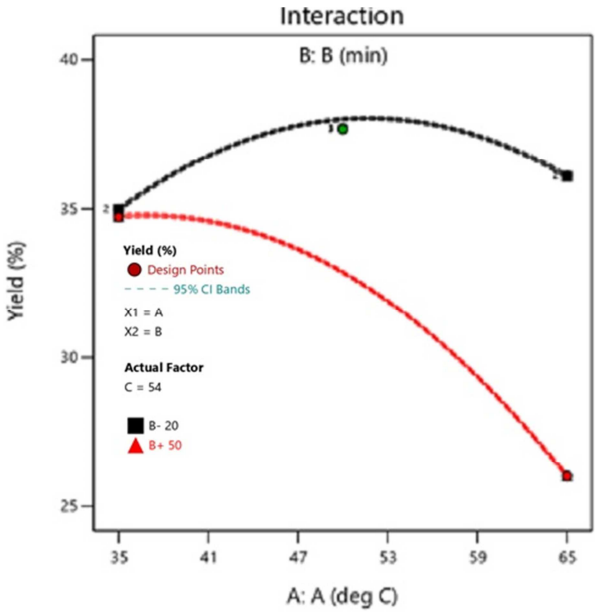

Figure 10. *Interaction effect of temperature and time on the yield.*

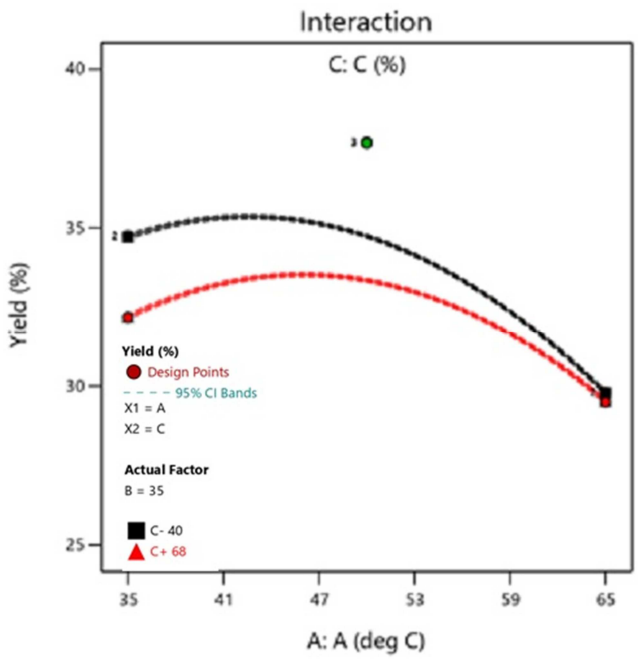

Figure 11. *Interaction effect of temperature and acid concentration on yield.*

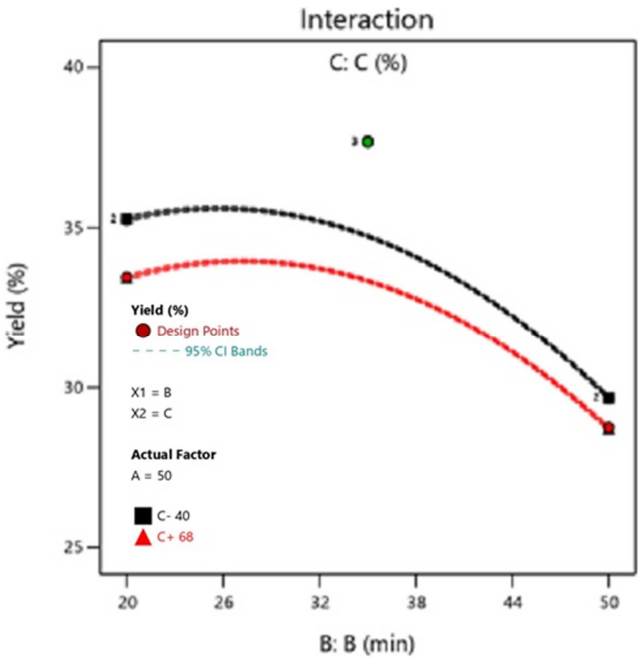

Figure 12. *Interaction effect of time and acid concentration on yield.*

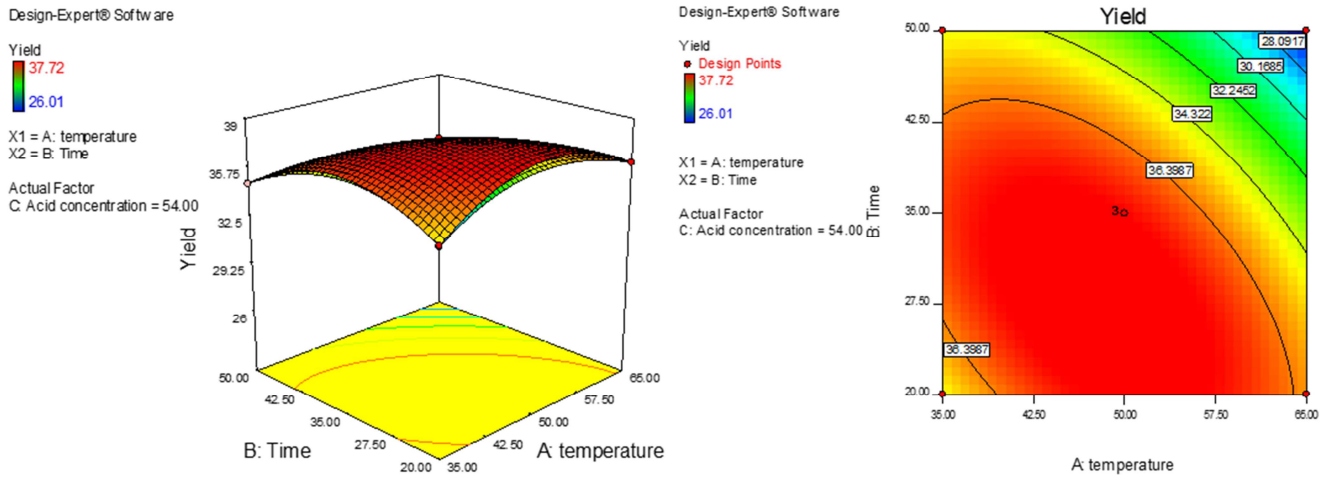

Figure 13. *Response surface and contour plot showing interaction effect of temperature and time on yield.*

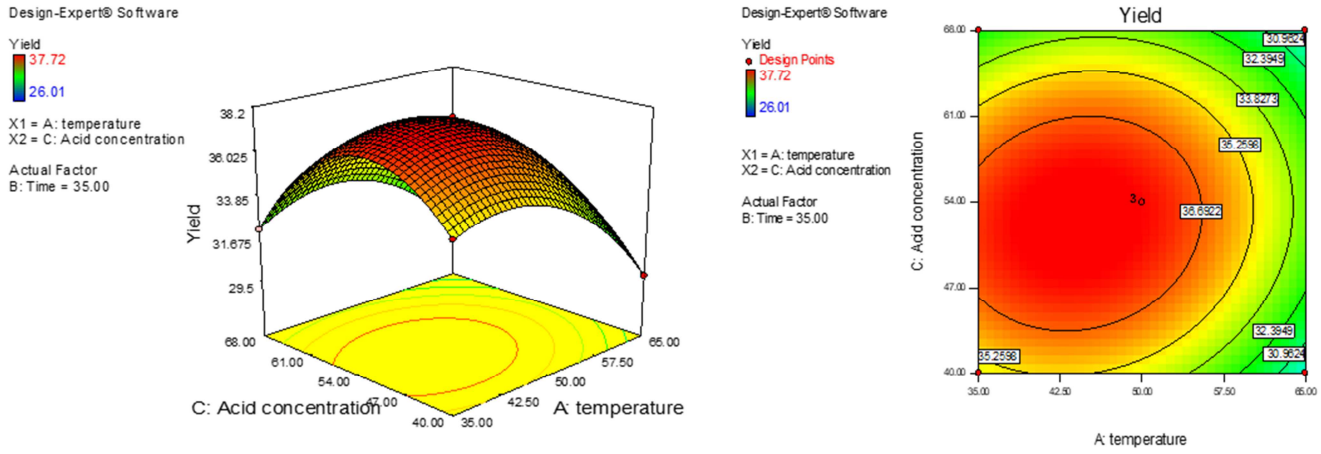

Figure 14. *Response surface and contour plot showing interaction of temperature and acid concentration.*

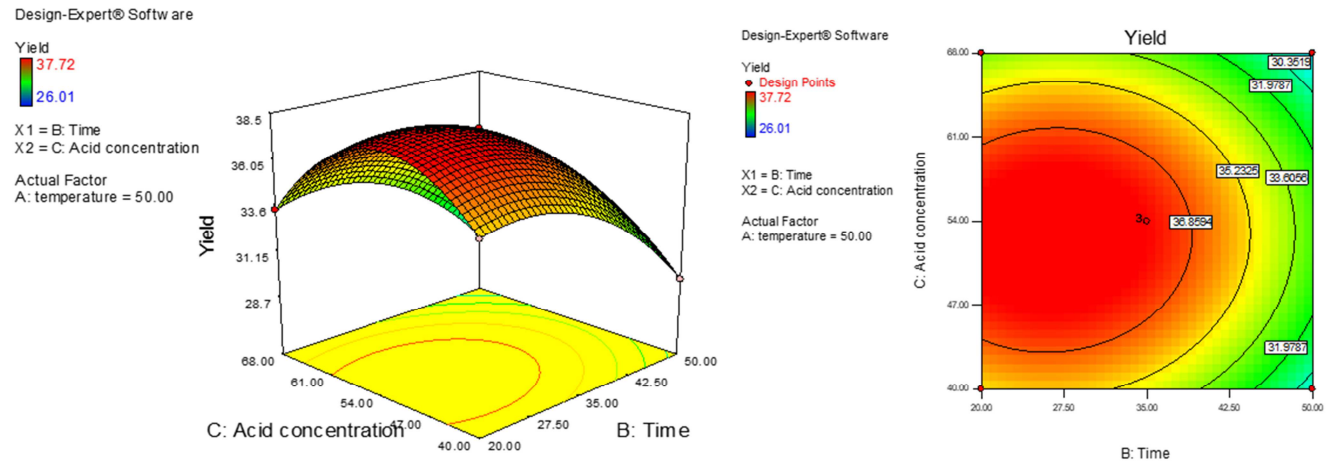

Figure 15. *Response surface and contour plot for time and acid concentration interaction.*

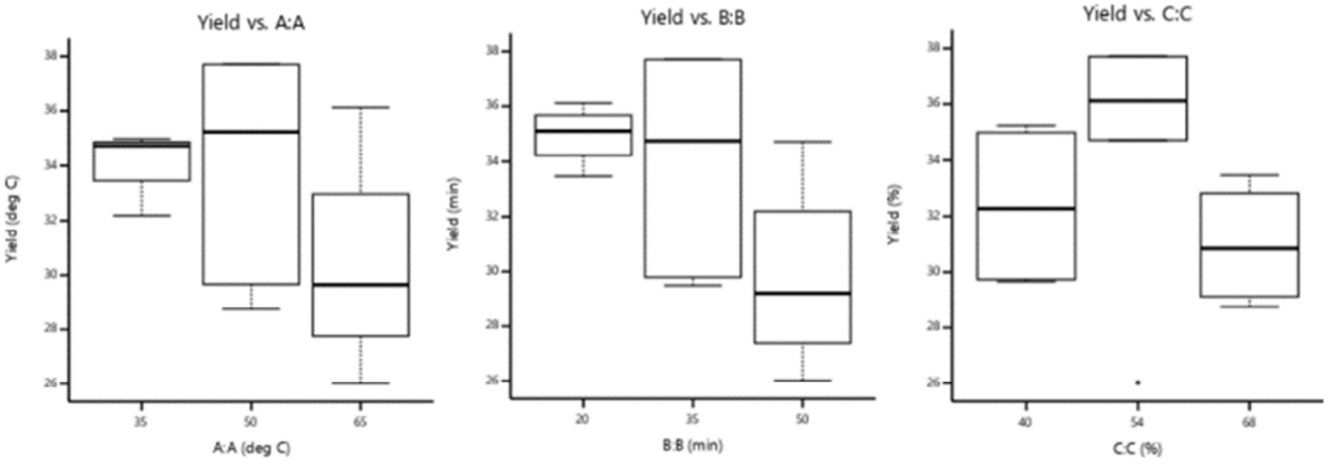

Figure 16. *Box Plot showing the response yield against (a) A: Temperature (b) B: Time (c) C: Acid Concentration.*

3.7.4. Box Plots

For visualization of experimental points and their effect on yield, box plots are shown in Figure 16, for standardized way of displaying the distribution of data based on a five number summary namely minimum, first quartile, median, third quartile and maximum. It helps to identify the data is symmetrical, how tightly grouped and its skewness. These parameters are well grouped and agree with conclusions drawn from interaction plots explained already.

3.7.5. Optimization of the of CNCs Yield

Optimization of the response surface is used to find the hydrolysis condition to obtain maximum CNCs yield. From the experimental result, a maximum yield of 37.72% was obtained at the interaction parameter of 50°C, 35 min and 54% of acid concentration. The predicted yield of CNCs obtained was 37.33%. From response optimization technique used in this study, the yield of CNCs was optimized to 38.40% at a desirable parameter interaction of 45.94°C, 26.94 min and 50.2% acid concentration.

4. Conclusion

Cellulose nanocrystalline (CNCs) was isolated from water hyacinth using acid hydrolysis methods. The extracted CNCs were characterized using SEM, FTIR, DSC, XRD and particle size analyzer. Extracted CNCs have whisker-shaped structure with an average diameter of 102.6 nm showing thermal stability. The effect of hydrolysis temperature, time and acid concentration on the yield of the CNCs were also investigated. The yield is negatively affected by temperature and time while acid concentration has positive effect on the yield. The experimental results show that a maximum yield of 37.72% can be obtained at 40°C, 45 min and 65% of acid concentration. Using RSM method the obtained result was optimized to 38.40% at 45.94°C, 26.94 min and 50.2% acid concentration.

The experience gained during this study related to synthesis of CNC, provide a new insight into its application and further research relating to effect of process parameters and significance of cellulose molecular weight.

Acknowledgements

The authors are grateful for the encouragement and support of The Dean, College of Engineering and Technology, The Academic Vice President, Bule Hora University, Bule Hora, Ethiopia and The Dean,

Biotechnology and Bioprocess Center of Excellence, Addis Ababa Science and Technology University, Addis Ababa, Ethiopia.

References

[1] Fatma Kallel, Fedia Bettaieb, Ramzi Khiari, Araceli García, Julien Bras, Semia Ellouz Chaabouni, (2016). Isolation and structural characterization of cellulose nanocrystals extracted from garlic straw residues. Industrial Crops and Products, 87, 287-296.

[2] Kristiina Oksman, Yvonne Aitomäki, Aji P. Mathew, Gilberto Siqueira, Qi Zhou, Svetlana Butylina, Supachok Tanpichai, Xiaojian Zhou, & Saleh Hooshmand, (2010). Review of the recent developments in cellulose nanocomposite processing. Composites Part A: Applied Science and Manufacturing, 83, 2-18.

[3] Endes, C., Camarero-Espinosa, S., Mueller, S., Foster, E. J., Petri-Fink, A., Rothen-Rutishauser, B., Weder, C., & Clift, M. J. D. (2016). A critical review of the current knowledge regarding the biological impact of nanocellulose. Journal of nanobiotechnology, 14 (1), 78.

[4] Hanieh Kargarzadeh, Marcos Mariano, Jin Huang, Ning Lin, Ishak Ahmad, Alain Dufresne, & Sabu Thomas (2017). Recent developments on nanocellulose reinforced polymer nanocomposites: A review. Polymer, 132, 368-393.

[5] João Paulo Saraiva Morais, Morsyleide de Freitas Rosa, Men de sá Moreira de Souza Filho, Lidyane Dias Nascimento, Diego Magalhães do Nascimento & Ana Ribeiro Cassales, (2013). Extraction and characterization of nanocellulose structures from raw cotton linter. Carbohydrate Polymers, 91 (1), 229-235.

[6] Ghazy, M. B., Esmail, F. A., El-Zawawy, W. K., Al-Maadeed, M. A., & Owda, M. E., (2016). Extraction and characterization of Nanocellulose obtained from sugarcane bagasse as agro-waste. Journal: Journal of Advances in Chemistry, 12 (3).

[7] Malucelli, L. Centa, Lacerda, L. Gustavo, Dziedzic, Maurício, da Silva Carvalho Filho, M. Aurélio (2017). Preparation, properties and future perspectives of nanocrystals from agro-industrial residues: a review of recent research. Reviews in Environmental Science and Bio/Technology, 16 (1), 131-145.

[8] Chirayil, C. J., L. Mathew & S. Thomas, (2014). Review of recent research in nano cellulose preparation from different lignocellulosic fibers, Reviews on advanced materials science, 37.

[9] Latif, M. H. A. & Y. F. Mahmood, (2018). Isolation and Characterization of Microcrystalline Cellulose and Preparation of Nano-Crystalline Cellulose from Tropical Water Hyacinth. Ibn AL-Haitham Journal for Pure and Applied Science, 31 (1), 180-188.

[10] Mashego, D. V., (2016). Preparation, isolation and characterization of nanocellulose from sugarcane bagasse. MSc Thesis, Durban University of Technology, Durban, South Africa.

[11] Börjesson, M., & Westman, G. (2015). Crystalline Nanocellulose — Preparation, Modification, and Properties. In M. Poletto, & H. L. O. Junior (Eds.), Cellulose - Fundamental Aspects and Current Trends. IntechOpen.

[12] Guo J, Du W, Wang S, Yin Y., & Gao Y., (2017). Cellulose nanocrystals: A layered host candidate for fabricating intercalated nanocomposites. Carbohydrate polymers, 157, 79-85.

[13] Tiffany Abitbol, Amit Rivkin, Yifeng Cao, Yuval Nevo, Eldho Abraham, Tal Ben-Shalom, Shaul Lapidot & Oded Shoseyov (2016) Nanocellulose, a tiny fiber with huge applications. Current opinion in biotechnology, 39, 76-88.

[14] Bhat, A. H., Dasan, Y. K., Khan, I., Soleimani, H., & Usmani, A. (2017). Application of nanocrystalline cellulose: Processing and biomedical applications. In Cellulose-Reinforced Nanofibre Composites: Production, Properties and Applications, 215-240, Elsevier.

[15] Patchiya Phanthong, Prasert Reubroycharoen, Xiaogang Hao, Guangwen Xu, Abuliti Abudula & Guoqing Guan, (2018). Nanocellulose: extraction and application. Carbon Resources Conversion, 1 (1), 32-43.

[16] Lee, H., S. B. A. Hamid & S. Zain, (2014). Conversion of lignocellulosic biomass to nanocellulose: structure and chemical process. The Scientific World Journal,

[17] Chen, Y., Wu, Q., Huang, B., Huang, M. & Ai, X. (2014). Isolation and characteristics of cellulose and nanocellulose from lotus leaf stalk agro-wastes. BioResources, 10 (1), 684-696.

[18] Jiang, F. & Y.-L. Hsieh, (2015). Cellulose nanocrystal isolation from tomato peels and assembled nanofibers. Carbohydrate Polymers, 122, 60-68.

[19] Roni Marcos dos Santos, Wilson Pires Flauzino Neto, Hudson Alves Silvério, Douglas Ferreira Martins, Noélio Oliveira Dantas, & Daniel Pasquini, (2013). Cellulose nanocrystals from pineapple leaf, a new approach for the reuse of this agro-waste. Industrial Crops and Products, 50, 707-714.

[20] Bich Thuyen Nguyen Thi, Luong H. V. Thanh, T. N. Phuong Lan, N. T. Dieu Thuy & Yi-Hsu Ju (2017). Comparison of some pretreatment methods on cellulose recovery from water hyacinth (Eichhornia crassipe). Journal of Clean Energy Technologies, 5 (4), 274-279.

[21] Sundari, M. T. & A. Ramesh, (2012). Isolation and characterization of cellulose nanofibers from the aquatic weed water hyacinth—Eichhornia crassipes. Carbohydrate Polymers, 87 (2), 1701-1705.

[22] Asrofi, M., Abral, H., Kasim, A., Pratoto, A., Mahardika, M., Park, Ji-Won & Kim, Hyun-Joong (2018). Isolation of nanocellulose from water hyacinth fiber (WHF) produced via digester-sonication and its characterization. Fibers and Polymers, 19 (8), 1618-1625.

[23] Asrofi, M., Abral, H., Kasim, A., Pratoto, A., Mahardika, M., & Hafizulhaq, F. (2018). Mechanical Properties of a Water Hyacinth Nanofiber Cellulose Reinforced Thermoplastic Starch Bionanocomposite: Effect of Ultrasonic Vibration during Processing. Fibers, 6 (2), 40.

[24] Sivasankari, B & R. David, (2016) A study on chemical analysis of water hyacinth (Eichornia crassipes), water lettuce (Pistia stratiotes). Int J Inno Res Sci Eng Technol, 5, 17566-17570.

[25] Priya, E. S., & P. S. Selvan, (2017). Water hyacinth (Eichhornia crassipes)–An efficient and economic adsorbent for textile effluent treatment–A review. Arabian Journal of Chemistry, 10, S3548-S3558.

[26] Raveendran Sindhu, Parameswaran Binod, Ashok Pandey, Aravind Madhavan, Jose Anju Alphonsa, Narisetty Vivek, Edgard Gnansounou, Eulogio Castro & Vincenza Faraco, (2017). Water hyacinth a potential source for value addition: an overview. Bioresource technology, 230, 152-162.

[27] Pitaloka, A. B., A. H. Saputra & M. Nasikin, (2013). Water hyacinth for superabsorbent polymer material. World Applied Sciences Journal, 22 (5), 747-754.

[28] Soetaredjo, F. E., Y.-H. Ju & S. Ismadji, (2016). Conversion of water hyacinth Eichhornia crassipes into biofuel intermediate: combination subcritical water and zeolite-based catalyst processes. Can Tho University Journal of Science special issue, Renewable Energy, 64-69.

[29] Wulandari, W., A. Rochliadi & I. Arcana. (2016). Nanocellulose prepared by acid hydrolysis of isolated cellulose from sugarcane bagasse. in IOP Conference Series: 107, 012045, Materials Science and Engineering. IOP Publishing.

[30] El Achaby M, Kassab Z, Aboulkas A, Gaillard C & Barakat A. (2018). Reuse of red algae waste for the production of cellulose nanocrystals and its application in polymer nanocomposites. Int J Biol Macromol. 106, 681-691.

[31] Kim, D.-Y., et al., Kim, Du-Yeong, Lee, Byoung-Min, Koo, Dong Hyun, Kang, Phil-Hyun, & Jeun, Joon-Pyo (2016). Preparation of nanocellulose from a kenaf core using E-beam irradiation and acid hydrolysis. Cellulose, 23 (5), 3039-3049.

[32] Thambiraj, S. & D. R. Shankaran, (2017). Preparation and physicochemical characterization of cellulose nanocrystals from industrial waste cotton. Applied Surface Science, 412, 405-416.

[33] Mariño M, Lopes da Silva L, Durán N, & Tasic L. (2015). Enhanced materials from nature: nanocellulose from citrus waste. Molecules. 20 (4), 5908-23.

[34] Amiralian, N., et al., Nasim Amiralian, Pratheep K. Annamalai, Paul Memmott, & Darren J. Martin (2015). Isolation of cellulose nanofibrils from Triodia pungens via different mechanical methods. Cellulose, 22 (4), 2483-2498.

[35] Chan, H. C., Chia, C. H., Zakaria, S., Ahmad, I., & Dufresne, A. (2012). Production and characterisation of cellulose and nano-crystalline cellulose from kenaf core wood. BioResources, 8 (1), 785–794.

[36] Liu C, Li B, Du H, Lv D, Zhang Y, Yu G, Mu X, & Peng H. (2016). Properties of nanocellulose isolated from corncob residue using sulfuric acid, formic acid, oxidative and mechanical methods. Carbohydr Polym., 151, 716-724.